

Short Isometric Shapelet Transform for Binary Time Series Classification

Weibo Shu, Yaqiang Yao, and Huanhuan Chen, *Senior Member, IEEE*

Abstract—In the research area of time series classification (TSC), ensemble shapelet transform (ST) algorithm is one of state-of-the-art algorithms for classification. However, the time complexity of it is often higher than other algorithms. Hence, two strategies of reducing the high time complexity are proposed in this paper. The first one is to only exploit shapelet candidates whose length is a given small value, whereas the ensemble ST uses shapelet candidates of all the feasible lengths. The second one is to train a single linear classifier in the feature space, whereas the ensemble ST requires an ensemble classifier trained in the feature space. This paper focuses on the theoretical evidences and the empirical implementation of these two strategies. The theoretical part guarantees a near-lossless accuracy under some preconditions while reducing the time complexity. In the empirical part, an algorithm is proposed as a model implementation of these two strategies. The superior performance of the proposed algorithm on some experiments shows the effectiveness of these two strategies.

Index Terms—Time Series Classification, Feature Selection, Feature Space, Machine Learning

I. INTRODUCTION

TIME series is one type of multidimensional data with a wide range of applications in economy, medical treatments, and engineering [1]. The ordered values in time series contain much latent information of data, which makes time series analysis a challenging task. Time series classification (TSC) plays a significant role in time series analysis. It appears in a number of new circumstances such as text retrieval [2], shape classification [3], and bioinformatics [4]. Therefore, many algorithms have been proposed to tackle TSC problems during the last decades.

The existing algorithms of TSC can be approximately divided into the following categories [5]. The first class of algorithms are based on the similarity between two whole time series. Several bespoke distance metrics between pairwise time series have been designed to measure the similarity between any two whole time series. And the classification is dependent on these specific distance metrics [6]–[14]. In contrast to the whole series similarity algorithms, another class of algorithms focus on extracting local features of time series to classify them [15]–[21]. There is a novel class of algorithms whose main idea is transforming time series into strings by a uniform dictionary and then measuring the similarity among these strings [22]–[26]. Model based algorithms represent time series with models and then conduct classification on these models [27]–[30]. Another competitive class of algorithms try to transform source data into a new feature space and then

classify them in the new feature space [31]–[36]. The last one are ensemble algorithms whose base classifiers are from the abovementioned categories [14], [16], [26], [35].

Among those algorithms, ensemble shapelet transform (ST) algorithm is one of state-of-the-art algorithms in terms of classification accuracy [5], [32], [33]. However, some redundancy of this algorithm causes a high time complexity. Some variants have been proposed to tackle this challenge. But most of them might downgrade the accuracy while reducing the time complexity.

To tackle the challenge, two strategies are proposed in this paper. The first strategy is to give a small fixed length and drop those shapelet candidates whose length is not the given one. It will largely reduce the number of shapelet candidates in the ensemble ST algorithm. The second one is to substitute the ensemble classifier with a single classifier in the shapelet-dependent feature space, which will sharply decrease the classifier training time. In addition, theoretical evidences to support the effectiveness of these two strategies will be given in this paper, which can guarantee the reduction of time complexity with the near-lossless accuracy achieved by the state-of-the-art on most of binary data sets. Besides, the short isometric shapelet transform algorithm is proposed as a model implementation of these two strategies. Some experiments on this algorithm will show advantages of the two proposed strategies.

The rest of the paper is organized as follows. The background and outline of the model implementation are in Section II. Theoretical analysis about the proposed strategies is in Section III. Section IV shows advantages of the proposed strategies and Section V is a conclusion.

II. SHORT ISOMETRIC SHAPELET TRANSFORM MODEL

A. Time shapelet

Firstly, two basic terminologies are introduced as follows:

time series data

One sample of the time series data set is an ordered m -dimensional vector with a class label. It is expressed with (\mathbf{x}, y) or \mathbf{x} , where \mathbf{x} is the ordered vector data and y is the class label. The whole data set is $(\mathbf{X}, \mathbf{Y}) = ((\mathbf{x}_1, y_1), (\mathbf{x}_2, y_2), \dots, (\mathbf{x}_n, y_n))$. In general, time series in a data set are isometric after the preliminary processing.

shapelet

The shapelet is the discriminative subseries derived from time series [19]. Subseries are continuous subsequences of time series. A shapelet is expressed with (s, z) or s ,

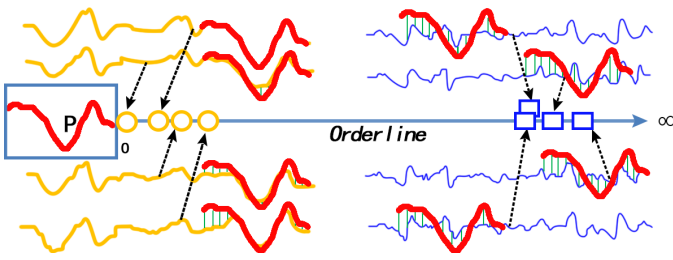


Fig. 1. This picture shows the real number axis of a shapelet candidate P . In this picture, shapelet candidate P in the blue box will be calculated the distance to any time series that are represented by the yellow and blue curves in the picture. ‘Orderline’ in the picture is the real number axis, and distances from P to each time series are marked on the axis. The yellow circles and blue boxes are used to mark the calculated distances on the real line for readers.

where s is the subseries and z is the class label from its original time series. In a shapelet-dependent algorithm, each shapelet usually represents a local feature of the data of one class.

The shapelet was proposed by Ye and Keogh, and they used shapelets to build a decision tree where the attribute of each tree node is the distance between time series and a selected shapelet [19].

Shapelets are selected from shapelet candidates that are all the subseries of all the time series in a data set. For a shapelet candidate, distances from it to each time series of a target set are calculated. After that, a prime segmentation is explored on the real number axis where all the calculated distances are marked. The real number axis before segmentation is shown in Fig 1 [37]. Then by classifying time series according to the divided segments which their corresponding distances fall in, time series in the target set are divided into some disjoint subsets. Subsequently, the information gain is calculated according to their entropy. Finally, shapelet candidates with better information gain are selected as shapelets.

Due to the substantial time consumption spent in selecting shapelets by brute force, Ye and Keogh exploited some tricks such as early abandon to reduce the time consumption [19]. Researchers also tried other methods to solve this time consumption problem [20], [21], [38]. Though to a certain extent time complexity has been reduced, there is some loss of accuracy.

B. Distance between shapelet and time series

In shapelet-dependent TSC algorithms, a basic manipulation is calculating the distance between time series and a shapelet. In most cases, shapelets are not as long as time series. Hence, the distance between a shapelet (s, z) and a time series (x, y) is usually calculated by the following formula [19]:

$$Dist(s, x) = \min \left\{ d(s, P) \mid \begin{array}{l} P = (x_i, \dots, x_{i+k-1}), \\ i = 1, \dots, m - k + 1 \end{array} \right\} \quad (1)$$

where $d(\cdot, \cdot)$ is the function of Euclidean Distance, P is the subseries which means the continuous subsequence, m is the length of time series x , and k is the length of shapelet s . This formula also serves as the distance calculation formula between shapelet candidates and time series. And the time complexity of a distance calculation is $\mathcal{O}(k(m - k))$.

C. Shapelet transform (ST)

Shapelet transform (ST) is an influential algorithm that uses shapelets as basis to construct a feature space [32]. It uses a disposable selection to select k shapelets from all the shapelet candidates. Then it transforms original time series into a k -dimensional vector where the value of the i th dimension is the distance between time series and the i th selected shapelet. Finally It carries out a classification in that feature space [32].

This method exploits shapelets in a different way from constructing a decision tree. The shapelet selection happens only once in this method, whereas it happens many times in constructing a decision tree. More precisely, in shapelet-dependent decision tree algorithms, the frequency of the shapelets selection equals the number of branch nodes in the decision tree. Hence, after this work, the key point of cutting time consumption has changed to selecting the most discriminative k shapelet candidates as fast as possible [39], [40]. However, the time complexity is still high as a result of the large number of shapelet candidates as well as the complex distance calculation.

To reduce the high time complexity, the short isometric shapelet transform (SIST) model is proposed in this paper and it will be introduced next.

D. Short isometric shapelet transform (SIST)

For clearly elucidating improvements by a comparison, the SIST algorithm will be introduced with the ensemble ST algorithm.

For a TSC problem, the first step of the ensemble ST algorithm is to extract all the subseries of each time series as shapelet candidates. But in the SIST algorithm, only the subseries with a small fixed length will be extracted from each time series. Therefore, the number of shapelet candidates in the SIST algorithm becomes fairly small compared with that in the ensemble ST algorithm. The validity of this strategy will be elaborated later. Step 1 of Fig 2 shows the difference.

The second step is to select shapelets from shapelet candidates. According to the elaboration in Subsection II-A, a process of exploring the prime segmentation in a real line is indispensable in this step. But in the SIST algorithm, this time-consuming process is removed by using the generalized Rayleigh quotient rather than the prime information gain as the discrimination index of shapelet candidates. Besides, the position of shapelet candidates in its original time series is exploited to simplify the distance calculation described in Subsection II-B. Moreover, these improvements will be justified later. And all these differences are shown in step 2 of Fig 2.

In the ensemble ST algorithm, the final step is to transform source time series into vectors by selected shapelets (the transformation is described in II-C) and then train an ensemble classifier in that vector space. But we claim that if shapelets are selected by using the generalized Rayleigh quotient of shapelet candidates as the selection priority, there is a high degree of the linear separability of the transformed data in the vector space. Consequently, a single SVM is enough to classify data well. Theoretical evidences to support this claim will be given

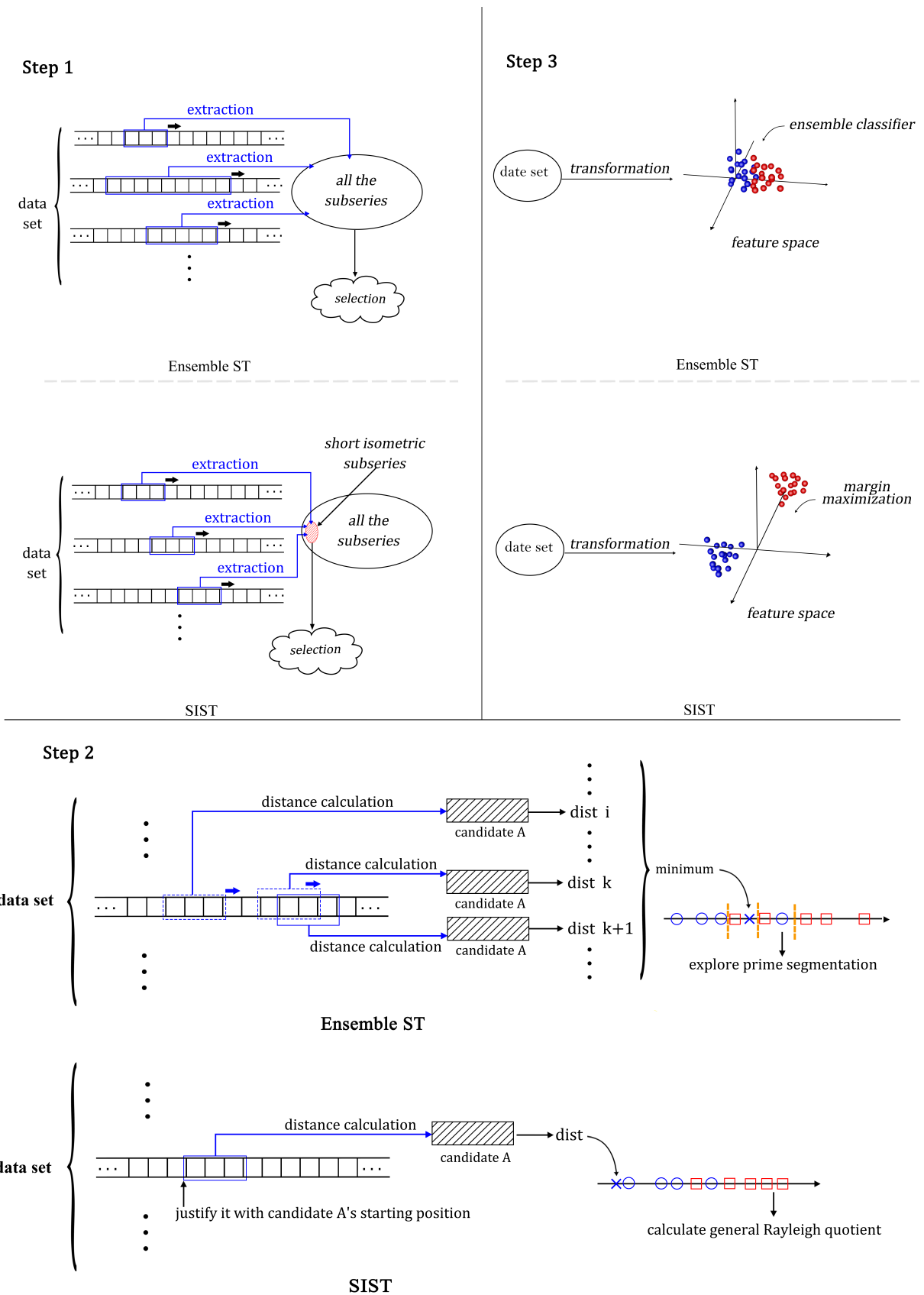


Fig. 2. Differences between the ensemble ST and the SIST. Details of this picture are discussed in Subsection II-D

later. Step 3 of Fig 2 shows the difference in the final step. Furthermore, since shapelets are short and distance calculation is simplified in the SIST algorithm, much time is saved in the time series transformation of the SIST algorithm.

III. THEORETICAL ANALYSIS

In this section, theoretical evidences of the proposed strategies will be elaborated. We reiterate the two strategies here. The first one is to give a small fixed length and drop those shapelet candidates whose length is not the given one. This strategy will largely reduce the number of shapelet candidates. The second one is to replace the ensemble classifier with a single SVM in the feature space, which will sharply cut the time consumption of the classifier training.

The theoretical evidences in this section can guarantee as small as possible loss of accuracy compared with largely reduced time complexity.

The contents of this section are organized as follows. Firstly, the shapelet candidate extraction based on the proposed ‘Fixed Distance’ will be analyzed in Subsection III-A and III-B. This part is about the theoretical evidences of the first proposed strategy. Subsequently, the rationality of substituting the ensemble classifier with a single linear classifier will be discussed in III-C. Finally, the concrete algorithmic flow with the time complexity analysis is given in Subsection III-D.

A. Simplification of the distance calculation

In typical shapelet-dependent algorithms, it is time-consuming to measure the distance between shapelets and time series. The high time complexity of one distance calculation is drastically amplified by the frequency of the distance calculation.

Hence a basic idea in this paper is to use the position information of shapelets to simplify the distance calculation shown in Eq. (1). Each shapelet or shapelet candidate is a subseries derived from an original time series in the data set. Therefore, its start point is a specific position in its original time series. The starting position can be used to simplify the distance calculation as the following ‘Fixed Distance’ shows.

$$Fixed_Dist(\mathbf{s}, \mathbf{x}) = \left\{ d(\mathbf{s}, P) \mid P = (x_i, \dots, x_{i+k-1}), \right. \\ \left. i = j \right\} \quad (2)$$

where j is the starting position of shapelet \mathbf{s} and other parameters are same with them in Eq. (1). It also serves as the distance calculation formula of shapelet candidates and time series. From Eq. (1) to Eq. (2), the time complexity of a distance calculation has been changed from $\mathcal{O}(k(m-k))$ to $\mathcal{O}(k)$.

Comparing Fixed Distance with the typical distance metric shown in Eq. (1), it can be found that Eq. (1) focuses only on whether a time series possesses the local feature represented by the shapelet, whereas Eq. (2) focuses not only on the existence of the local feature in a time series, but also on the position where the local feature appears in a time series. Moreover, if distances between shapelets and time series are calculated by Eq. (2), much time is saved. One part of the saved time

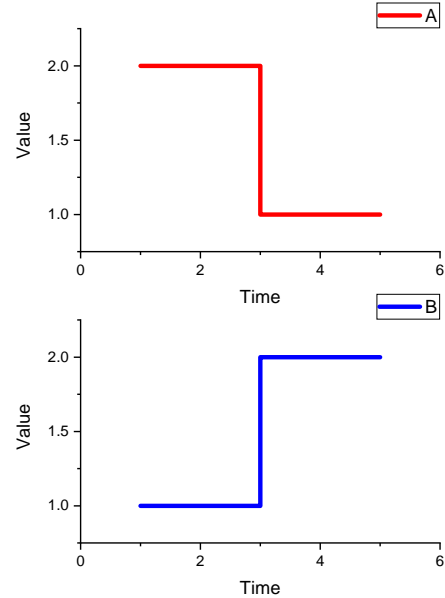


Fig. 3. Example of the usage of position information. The first half of class A can distinguish A and B by Eq. (2), whereas it can not do that by Eq. (1).

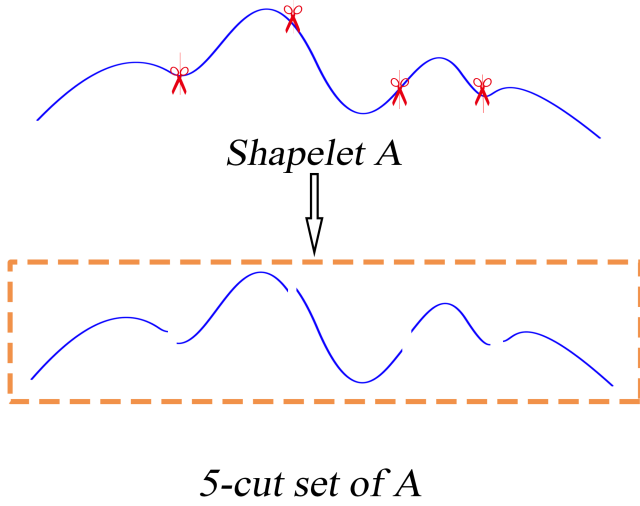
is evident from the comparison between Eq. (1) and Eq. (2). The other part is indirect, and details will be elaborated in Subsection III-B. In that subsection, Fixed Distance plays an important role.

There is a simple example illustrating that Eq. (2) reinforces the discrimination ability of shapelets. Data A and B are shown in Fig 3. If the first half of class A is selected as a shapelet S , then by Eq. (1), the distance between S and A is 0 and the distance between S and B is also 0. However, if distances are calculated by Eq. (2), then the distance between S and A is 0 and the distance between S and B is $\sqrt{2}$. Hence, S can classify A and B by Eq. (2) whereas it can not do that by Eq. (1). That is because in Eq. (2), the distance calculation takes into account the position of the local feature represented by the shapelet. In Eq. (2), the distance calculation is fixed at the specific position marked by the start point of the shapelet. That’s why it is called ‘Fixed Distance’.

B. Short isometric shapelet candidates

In this subsection, theoretical analysis focuses on fixing the length of shapelet candidates, namely the strategy showed in Step 1 of Fig 2.

In the process of selecting appropriate shapelets, the time of evaluating a single shapelet candidate is multiplied by the number of all the shapelet candidates. And the number of shapelet candidates is so substantial that the time consumption is huge. If it can be known about the prime length or even a small range of the prime length of shapelets, then shapelet candidates whose length are not the prime one can be discarded. And the huge time consumption vanishes as a result of the drastic reduction of the number of shapelet candidates. Generally speaking,


 Fig. 4. Example of n -cut set

it is hard to know the prime length, or the time spent in searching the best length is not less than the time it saves. However, in the ST algorithm, under the precondition that Fixed Distance is used as the distance calculation formula, the length of shapelet candidates can actually be fixed without an appreciation of the prime length. To explain this conclusion, firstly some conceptions should be strictly defined as follows:

Definition 1. Giving a n -size set A of time series and a k -size set B of shapelets, the process of transforming each time series in A into a k -dimensional vector by metric d , which means the value at the i th dimension of the k -dimensional vector is the d metric from the time series to the i th shapelet in B , is called A 's **shapelet transform through B by metric d** .

Definition 2. Giving a shapelet (s, z) , cut it in arbitrary $n - 1$ cut points to produce n ($n > 1$) subseries of (s, z) . Each subseries is a new shapelet derived from (s, z) and all of them constitute (s, z) . The set of the n new shapelets is called the **n -cut set** of (s, z) .

A simple example of n -cut set is shown in Fig 4. Based on the abovementioned conceptions, a key proposition is given as follows:

Proposition 1. A is a vector set coming from a time series set B 's shapelet transform through a single shapelet (s, z) by Fixed Distance, and C is another vector set coming from B 's shapelet transform through D by Fixed Distance too, here D is an arbitrary n -cut set of (s, z) with any $n > 1$. Then for any time series in B , its corresponding vector in A has the

same Euclidean norm with its corresponding vector in C .

Proof. For any time series (x, y) in set B , what is needed is to prove that its shapelet transform through (s, z) by Fixed Distance has the same Euclidean norm with its shapelet transform through any n -cut set D of (s, z) by Fixed Distance.

The following are the formulation of the time series x , the shapelet s and the n -cut set D .

$$\mathbf{x} = (x_1, x_2, \dots, x_m) \quad (3a)$$

$$\mathbf{s} = (s_i, s_{i+1}, \dots, s_{i+k}) \quad 1 \leq i \leq m, \quad i+k \leq m \quad (3b)$$

$$D = \{\mathbf{s}_1, \mathbf{s}_2, \dots, \mathbf{s}_n\} \quad 1 \leq n \leq k+1 \quad (3c)$$

$$t_j = \text{the terminal position of } \mathbf{s}_j \quad (3d)$$

$$1 \leq j \leq n, \quad i \leq t_1 < t_2 < \dots < t_n = i+k$$

$$\mathbf{s}_1 = (s_i, s_{i+1}, \dots, s_{t_1}) \quad (3e)$$

$$\mathbf{s}_h = (s_{t_{h-1}+1}, s_{t_{h-1}+2}, \dots, s_{t_h}) \quad 2 \leq h \leq n \quad (3f)$$

Next formulas represent the vectors transformed through s and D respectively by Fixed Distance.

$$V_{\mathbf{x}/\mathbf{s}} = \left(\sqrt{\sum_{p=i}^{i+k} (x_p - s_p)^2} \right) \quad (4)$$

$$V_{\mathbf{x}/D} = \left(\sqrt{\sum_{p=i}^{t_1} (x_p - s_p)^2}, \sqrt{\sum_{p=t_1+1}^{t_2} (x_p - s_p)^2}, \dots, \sqrt{\sum_{p=t_{n-1}+1}^{t_n} (x_p - s_p)^2} \right) \quad (5)$$

The next step is to prove that these two vectors have the same Euclidean norm. Noticing that if all the shapelets in D are concatenated in sequence then the shapelet s is acquired, hence:

$$\begin{aligned} \|V_{\mathbf{x}/D}\|_2 &= \sqrt{\sum_{p=i}^{t_1} (x_p - s_p)^2 + \sum_{q=2}^n \sum_{p=t_{q-1}+1}^{t_q} (x_p - s_p)^2} \\ &= \sqrt{\sum_{p=i}^{t_n} (x_p - s_p)^2} \\ &= \sqrt{\sum_{p=i}^{i+k} (x_p - s_p)^2} \\ &= \|V_{\mathbf{x}/\mathbf{s}}\|_2 \end{aligned} \quad (6)$$

And this is exactly what is needed. \square

According to the shapelet transform defined in Definition 1, the word 'norm' in the Proposition 1 actually means the similarity measurement between the time series and the shapelets representing a local feature set of the class ' z '. Therefore, in Proposition 1, for a very discriminative shapelet (s, z) , the Euclidean norm of a corresponding vector of the time series whose class label is ' z ' should be as small as possible, and it of the other vectors should be as large as possible (Here, the small

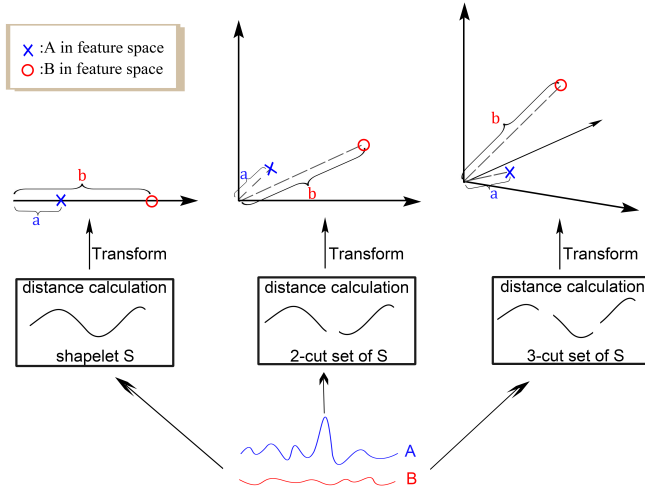


Fig. 5. An intuitive example to interpret Proposition 1. A and B are two time series, and they are transformed through a shapelet, its 2-cut set, and its 3-cut set respectively by Fixed Distance. Though A have different representative vectors in different feature spaces, they both keep the same length (the Euclidean norm) in different feature spaces. And so does B. Hence one keeps close to origin and the other keeps far from origin in all the three feature spaces.

value of similarity measurement means a high similarity and the big one means a low similarity). Hence, this proposition actually ensures that the similarity measurement is an invariant under those two different shapelet transform processes. An intuitive and simple example is shown in Fig 5.

Furthermore, the following corollary can be proved based on Proposition 1.

Corollary 1. *A* is a vector set coming from a time series set *B*'s shapelet transform through a shapelet set *C* by Fixed Distance, $D \subset C$, $E = \bigcup_{s \in D} (n_s\text{-cut set of } s)$, and $F = C - D \cup E$. *G* is another vector set coming from *B*'s shapelet transform through *F* by Fixed Distance. Then for any time series in *B*, its corresponding vector in *A* has the same Euclidean norm with its corresponding vector in *F*.

Proof. The proof begins with the following notation. *C* is a shapelet set represented as follows:

$$C = \{s_1, s_2, \dots, s_m\} \quad (7)$$

and *D* is a subset of *C*, it is represented as follows:

$$D = \{s_{k_1}, s_{k_2}, \dots, s_{k_l}\} \quad (8)$$

E, as defined in the corollary, is the union set of all the n_s -cut sets of shapelets in *D*, and it is represented as follows:

$$E = \{s_{k_1}^1, \dots, s_{k_1}^{n_{k_1}}, s_{k_2}^1, \dots, s_{k_2}^{n_{k_2}}, \dots, s_{k_l}^1, \dots, s_{k_l}^{n_{k_l}}\} \quad (9)$$

Besides, $C - D$ is represented as follows:

$$C - D = \{s_{t_1}, s_{t_2}, \dots, s_{t_{m-l}}\} \quad (10)$$

Hence, a time series *x*'s shapelet transform through *C* and $C - D \cup E$ respectively by Fixed Distance are as follows:

$$V_{x/C} = \left(\begin{array}{c} \|V_{x/s_{k_1}}\|_2, \dots, \|V_{x/s_{k_l}}\|_2, \\ \|V_{x/s_{t_1}}\|_2, \dots, \|V_{x/s_{t_{m-l}}}\|_2 \end{array} \right) \quad (11)$$

$$V_{x/C-D \cup E} = \left(\begin{array}{c} \|V_{x/s_{k_1}^1}\|_2, \dots, \|V_{x/s_{k_1}^{n_{k_1}}}\|_2, \\ \dots \\ \|V_{x/s_{k_l}^1}\|_2, \dots, \|V_{x/s_{k_l}^{n_{k_l}}}\|_2, \\ \|V_{x/s_{t_1}}\|_2, \dots, \|V_{x/s_{t_{m-l}}}\|_2 \end{array} \right) \quad (12)$$

Now calculate Euclidean norm of these two vectors:

$$\begin{aligned} \|V_{x/C}\|_2 &= \sqrt{\sum_{p=1}^l \|V_{x/s_{k_p}}\|_2^2 + \sum_{q=1}^{m-l} \|V_{x/s_{t_q}}\|_2^2} \\ &= \sqrt{\sum_{p=1}^l \sum_{r=1}^{n_{k_p}} \|V_{x/s_{k_p}^r}\|_2^2 + \sum_{q=1}^{m-l} \|V_{x/s_{t_q}}\|_2^2} \\ &= \|V_{x/C-D \cup E}\|_2 \end{aligned} \quad (13)$$

The second equal sign is hold by Proposition 1. And this finishes the proof of Corollary 1. \square

According to this corollary and the analysis tightly after Proposition 1, if the approximate n -cut set of a shapelet (s, z) is added as part of the shapelet basis used for the shapelet transform, then (s, z) in itself can be dropped in that shapelet basis. That's because the classification in the feature space mainly relies on the similarity measurement between transformed data and selected local features. However, the shapelet transform reflects the similarity measurement on the norm of transformed vectors, and Corollary 1 guarantees the identical norms of transformed vectors in feature spaces constructed by the two different shapelet basis. Hence, Corollary 1 actually says that the original shapelet basis and the changed shapelet basis can construct the nearly same feature space in terms of classification. Therefore, in a shapelet basis, the substitution of a shapelet with its n -cut set is feasible while the eventual purpose is classifying transformed data.

Every long shapelet consists of some short shapelets so that it must have an n -cut set including only short sub-shapelets. As stated above, Corollary 1 guarantees that all the shapelets can be replaced by their cut sets of short sub-shapelets. Therefore, selecting the elementary short shapelets is quite enough. Hence, the length of shapelet candidates can be fixed at a small number and these shapelet candidates are called 'short isometric shapelet candidates'.

After restricting the length of shapelet candidates to a small constant h , the number of shapelet candidates is cut to $n(m - h + 1)$ for a n -size and m -length time series set while there are $\frac{nm(1+m)}{2}$ shapelet candidates in typical shapelet-dependent algorithms.

C. Substituting the ensemble classifier in the feature space

After extracting short isometric shapelet candidates, the next step is to select shapelets from these short isometric shapelet candidates. This subsection begins at the analysis of the selection of shapelets. Since it is the key point of substituting the ensemble classifier in the shapelet-dependent feature space.

As previously mentioned, in the process of selecting shapelets from shapelet candidates, if the prime information gain is used as the discrimination index of shapelet candidates, then the evaluation of a shapelet candidate can not get rid of searching a prime segmentation for data represented in a real number axis (see Subsection II-A). And this operation is time-consuming.

On the other hand, the selected shapelets are also relevant to the distribution of transformed time series in the feature space. If nothing can be ensured of this distribution in the feature space, things become fairly complicated. The following illustration is shown to explain this point.

In the ensemble shapelet transform algorithm, the classifier is often an ensemble one of almost all kinds of typical classifiers trained in the feature space. It costs much time to train such an elaborate ensemble classifier. However, it is necessary to do that on account of the uncertainty of the distribution of data in the feature space. In that algorithm, each base classifier tries to catch one possible distribution of data in the feature space, while using the single classifier must undertake the risk of misestimating the data distribution. One radical cause of that plight is that the discrimination index of shapelets is designed without a thought about the combination of shapelets. That is to say, mere good separability in each dimension ensures little in the total space.

This illustration exemplifies that considering more than discrimination of a single shapelet is required while selecting shapelets from shapelet candidates. The combination of shapelets is another important issue while selecting shapelets. If the selected shapelet set constructing the feature space can ensure a linear separability of the data distribution, the classification conducted in the feature space will become comparatively easy. In the Euclidean feature space constructed by the shapelet transform, each shapelet represents a dimension, and values in that dimension represent the distance to the shapelet. If projections of transformed data onto each dimension is completely separable, which means there is a cut line completely dividing data from different class, the transformed data can be surely linearly separable in the total space. However, in practice, the majority of axes is the one where the projection onto it can not be completely divided, even though shapelets are selected as discriminative as they can. Hence, the difficulty is to ensure a high degree of linear separability while projections of data onto a single axis can not be completely divided. Thanks to the next Proposition 2, this goal can be achieved by using the generalized Rayleigh quotient as the selection priority of shapelet candidates.

Before stating and proving Proposition 2, the generalized Rayleigh quotient used in this paper should be defined. For two different classes of data distributed on a single real axis,

the generalized Rayleigh quotient is calculated by the next formula:

$$GRQ(A, B) = \frac{|\mu(A) - \mu(B)|}{\sigma^2(A) + \sigma^2(B)} \quad (14)$$

where GRQ is a short hand of ‘generalized Rayleigh quotient’, $\mu(\cdot)$ is the function to get the mean value, and $\sigma^2(\cdot)$ is the function to get the variance. For the shapelet candidate in a binary TSC problem, after building the real number axis shown in Fig 1, Eq. (14) can be used to calculate the GRQ value.

The next part is the statement and the proof of the crucial Proposition.

Proposition 2. For a binary TSC problem in a Euclidean feature space constructed by the shapelet transform, the generalized Rayleigh quotient of the projections of transformed data onto any single axis has a positive correlation with the degree of the linear separability of the transformed data.

Proof. Firstly, some notations are necessary:

$X \setminus Y \setminus X' \setminus Y'$: a real random vector
Ω	: set of all real random vectors
$\mu : \Omega \mapsto \cup_{k=1}^{\infty} R_k$: a function getting the mean vector of the random vector
$\mu_j : \Omega \mapsto R$: a function equals to $\pi_j \circ \mu$ where π_j is a projection map which gets the value of a vector's j -th dimension
$[\]^2$: get a vector which the value of each dimension equals the square of the original value
$\sigma^2 : \Omega \mapsto \cup_{k=1}^{\infty} R_k$: a function getting the diagonal vector of the covariance matrix of the random vector
$\sigma_j^2 : \Omega \mapsto R$: a function equals to $\pi_j \circ \sigma^2$ where π_j is a projection map which gets the value of a vector's j -th dimension
$\Sigma_{X \setminus Y \setminus X' \setminus Y'}$: the covariance matrix of the random vector
LS	: the degree of the linear separability of vectors of two different classes

Based on the above notations, the proof can start. Assume that there are two time series classes whose corresponding sets are A and B , a shapelet set C whose cardinality is k . A 's shapelet transform through C by some metric (see definition 1) forms the sample set of a k -dimensional real random vector X . The same process of B forms the sample set of a k -dimensional real random vector Y . By the central

limit theorem, these two random vectors can be presumed to be independent spherical normally distributed. That is:

$$X \sim N(\mu(X), \Sigma_X) \quad (15)$$

$$Y \sim N(\mu(Y), \Sigma_Y) \quad (16)$$

And we naturally define the degree of the linear separability by the following formula:

$$LS = \max_{\mathbf{w}} P((X - Y) \cdot \mathbf{w} > 0) \quad (17)$$

$$\|\mathbf{w}\| = 1, \mathbf{w} \in R_k$$

Now for proving Proposition 2, it is just needed to prove that $|\mu_j(X) - \mu_j(Y)|$ has a positive correlation with LS and $\sigma_j^2(X) + \sigma_j^2(Y)$ has a negative correlation with LS for any j in scope.

For a fixed \mathbf{w} , the following result can be deduced by the previous conditions.

$$(X - Y) \cdot \mathbf{w} \sim N((\mu(X) - \mu(Y)) \cdot \mathbf{w}, (\sigma^2(X) + \sigma^2(Y)) \cdot [\mathbf{w}]^2) \quad (18)$$

For the prime normal vector \mathbf{w} of Eq. (17), it has that:

$$(\mu(X) - \mu(Y)) \cdot \mathbf{w} \geq 0 \quad (19)$$

$$(\mu_j(X) - \mu_j(Y)) \cdot \mathbf{w}_j \geq 0 \quad 1 \leq j \leq k \quad (20)$$

For the first inequality, that is because \mathbf{w} can be substituted with $-\mathbf{w}$ if the inequality does not hold. Then $-\mathbf{w}$ is better than \mathbf{w} , which contradicts that \mathbf{w} is the prime normal vector. It is the same with the second inequality, if it is less than 0, just substitute \mathbf{w}_j with $-\mathbf{w}_j$ to get a better normal vector \mathbf{w}' . And it contradicts that \mathbf{w} is the prime normal vector.

Assuming that the best LS and the prime normal vector \mathbf{w} have been acquired, if substitute X and Y with X' and Y' which are same with X and Y except for a specific j where $|\mu_j(X') - \mu_j(Y')| > |\mu_j(X) - \mu_j(Y)|$, then the following results hold from Eq. (18), (19) and (20).

$$\mu((X' - Y') \cdot \mathbf{w}') > \mu((X - Y) \cdot \mathbf{w}) \geq 0 \quad (21)$$

$$\sigma^2((X' - Y') \cdot \mathbf{w}') = \sigma^2((X - Y) \cdot \mathbf{w}) \quad (22)$$

Here \mathbf{w}' equals \mathbf{w} on all dimensions except for the j -th value. And $\mathbf{w}'_j = \text{sign}((\mu_j(X') - \mu_j(Y')) \cdot (\mu_j(X) - \mu_j(Y))) \cdot \mathbf{w}_j$, which aims to make $(\mu_j(X') - \mu_j(Y')) \cdot \mathbf{w}'_j$ positive. Combining with (17), they shows that:

$$LS' \geq P((X' - Y') \cdot \mathbf{w}' > 0) > P((X - Y) \cdot \mathbf{w} > 0) = LS \quad (23)$$

Fig 6 shows that situation. And this means that $|\mu_j(X) - \mu_j(Y)|$ has a positive correlation with LS for arbitrary j in scope.

Similarly, keep the assumption that the best LS and the prime normal vector \mathbf{w} of the optimization problem 17 have been acquired, and substitute X and Y with X' and Y' which are same with X and Y except for a specific j where $\sigma_j^2(X') + \sigma_j^2(Y') < \sigma_j^2(X) + \sigma_j^2(Y)$, then the following results hold from Eq. (18):

$$\mu((X' - Y') \cdot \mathbf{w}) = \mu((X - Y) \cdot \mathbf{w}) \geq 0 \quad (24)$$

$$\sigma^2((X' - Y') \cdot \mathbf{w}) < \sigma^2((X - Y) \cdot \mathbf{w}) \quad (25)$$

Combining with (17), Eq. (23) holds too. Fig 7 shows that

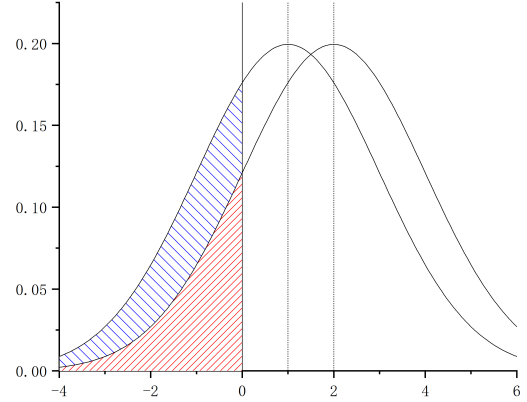


Fig. 6. Illustration of Eq. (23) (part I). Two independent normally distributed variables with positive means and the identical variance. The one whose mean is larger has a higher probability of being positive than the other. That's because the area under two curves are both 1 and the curve with the larger positive mean possesses a smaller area left to $x = 0$. Hence the curve with the larger positive mean has a larger area right to $x = 0$, which means a higher probability of getting a positive value.

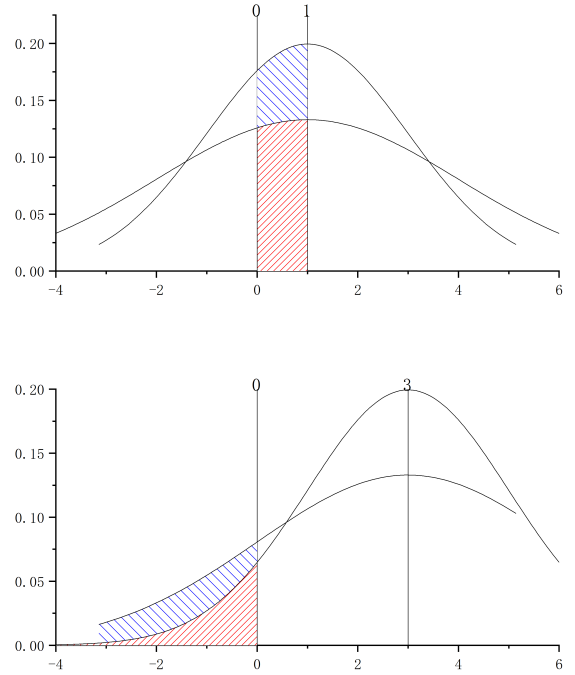


Fig. 7. Illustration of Eq. (23) (part II). For two independent normally distributed variables with the identical positive mean, the one whose variance is smaller has a higher probability of being positive than the other. There are two situations. The first one is that the left intersection point of two curves is left to $x = 0$, which is shown in the first picture. The second one is that the left intersection point of two curves is right to $x = 0$, which is shown in the second picture.

situation. And this means that $\sigma_j^2(X) + \sigma_j^2(Y)$ has a negative

correlation with LS for arbitrary j in scope. Then the proof of Proposition 2 is completed. \square

From the calculation formula of the GRQ (Eq. (14)), it can be seen that the GRQ surely has the ability to quantify the separation extent of data in a real number axis. Hence the large GRQ value ensures the discrimination of a single selected shapelet. The prime information gain also has this ability. But the large GRQ value in each single axis can ensure a high degree of the linear separability in the total space, whereas the large prime information gain can not do that. And this is exactly what Proposition 2 states. This property of the GRQ is the most important advantage of it compared with the prime information gain.

In Proposition 2, each axis of the feature space actually corresponds to the real number axis of a shapelet (the real number axis is shown in Fig 1). And the projections of transformed time series onto each axis are actually the distances from time series to the corresponding shapelet. Hence, Proposition 2 can ensure a high degree of the linear separability of data in the feature space under the precondition of selecting shapelets with the large GRQ value. As a result, if shapelets are selected according to the rank of GRQ values, training a single SVM to classify data also works at most cases. Once the ensemble classifier is substituted with a single SVM, time consumption is largely reduced for the reduction of training costs. Moreover, using the GRQ as the selection priority of shapelet candidates also successfully gets rid of the time-consuming operation that searching the best segmentation for different data in a real number axis.

D. Outline and Time Complexity of Training the SIST model

Considering the small delay which may happen in time series, a small relaxation is added to Eq. (2):

$$\text{Relaxed_Fixed_Dist}(\mathbf{s}, \mathbf{x}) = \min \left\{ d(\mathbf{s}, P) \left| \begin{array}{l} P = (x_{i_1}, \dots, x_{i_k}), \\ i_1 < i_2 < \dots < i_k < j + k + r, \\ -l \leq i_1 - j \leq r, \\ 1 \leq i_1 \leq \text{Len}(\mathbf{x}) - k + 1 \end{array} \right. \right\} \quad (26)$$

where both l and r are very small relaxation constants, P is the ordered subsequence which can be continuous or discontinuous, $\text{Len}(\cdot)$ is the function to get the length of time series, and other parameters are same with them in Eq. (2).

The algorithmic outline of training the SIST model is given in Algorithm 1.

For a data set D of n time series of length m , fixing the length of shapelet candidates at k , the time consumption of training the SIST model can be estimated as follows:

$$\begin{aligned} T(\text{SIST}) &= \mathcal{O}(n(m-k+1)T(SP) + T(R) + T(\text{SVM})) \\ &\approx \mathcal{O}(n^2mk + nm \log(nm) + Nn^2) \\ &= \mathcal{O}(n^2 \max(mk, N)) \\ &< \mathcal{O}(n^2m^2) \end{aligned} \quad (27)$$

Algorithm 1 Train the SIST classifier

Input: D the binary data set, L the shapelet length, r_a the left relaxation factor, r_b the right relaxation factor, N the number of shapelets

Output: Shapelet set S whose cardinality is N , a SVM classifier C with the linear kernel

- 1: initialize a null set T ;
- 2: **for** each time series $t \in D$ **do**
- 3: initialize a L -length shapelet candidate set T_t by a L -length window sliding from the initial point to the end point of t with step length 1;
- 4: $T = T \cup T_t$;
- 5: **end for**
- 6: initialize a priority queue S ;
- 7: **for** each shapelet candidate $s \in T$ **do**
- 8: **for** each time series $t \in D$ **do**
- 9: calculate Relaxed Fixed Distance between s and t by Eq. (26);
- 10: **end for**
- 11: calculate the generalized Rayleigh quotient of s by the calculated distances and Eq. (14);
- 12: set the generalized Rayleigh quotient as the priority of s ;
- 13: $S = S \cup s$;
- 14: **end for**
- 15: S =subqueue of S from position 0 to $N - 1$
- 16: do D 's shapelet transform through S by Relaxed Fixed Distance (the process is stated in definition 1) and get a vector set Ω ;
- 17: train a SVM C with linear kernel in Ω ;

where $T(SP)$, which is multiplied by the number of shapelet candidates, means the time complexity of calculating the selection priority of shapelet candidates, $T(R)$ means the time complexity of ranking all the shapelet candidates, and $T(\text{SVM})$ means the time complexity of training a SVM with the linear kernel in the feature space. Since the transformed vectors can be acquired in the process of calculating the selection priority, there is no extra time needed for the shapelet transform based on the selected shapelet basis. Empirically, N , which is the dimension of the feature space, is set less than m^2 . And k is obviously less than m . Therefore, the inequality is satisfied. And in the ensemble ST algorithm, the time complexity is $\mathcal{O}(n^2m^4)$ [32], [33]. This time complexity analysis shows some time complexity advantages of the proposed strategies. And in the next section, some experimental evidences of the advantages are given.

IV. EXPERIMENTAL EVIDENCES

A. Compared algorithms and Datasets

To show the advantages of the proposed strategies, the SIST model is compared with the state-of-the-art. According to the research of A. Bagnall et al., the following eight algorithms are to date the state-of-the-art algorithms [5]. They are COTE (Collection of Transformation Ensembles) [34], ST (ensemble edition) [33], BOSS (Bag of SFA Symbols, ensemble edition)

[26], EE (Elastic Ensemble) [14], DTWF (Dynamic Time Warping Features) [31], TSF (Time Series Forest) [16], TSBF (Time Series Bag of Features) [17], and LPS (Learned Pattern Similarity) [18].

The proposed model has some hyperparameters to be selected, and Table I shows the hyperparameter sets used in experiments. Line 1 is about whether removing the overlap shapelets. The item ‘true’ means that if two shapelets overlap, then the one with the lower selection priority is removed. And this choice may make the final shapelet number be smaller than the target number. This item means each discriminative position in a time series is at most once selected for classification. It is to say, users want a balance among every discriminative position’s contribution to classification in case that one position’s information covers others. The choice ‘false’ is just the opposite, which means users want to see that the more discriminative the position is, the stronger effects it has on the classification. Line 2 is about the length of shapelet candidates since only the short isometric shapelet candidates are extracted. Hyperparameters in line 3 decide the relaxation extent of the Fixed Distance calculation. Line 4 is about the number of shapelets used for the shapelet transform.

As for data sets, only the binary data sets from UCI data sets are selected, because Eq. (14) is restricted on binary TSC problems. In principle, for a multiclass TSC problem, the ‘one vs all’ strategy can solve it. However, the time complexity will be multiplied by the number of classes under this strategy. Hence, the ‘one vs all’ strategy may be not a good method for using the proposed strategies in a multiclass TSC problem. Multiclass TSC problems have a different structure from binary TSC problems, and this is another issue needing to be explored rather than tackled by a simple ‘one vs all’ strategy. Actually, the future work of this paper is regarding to expanding the proposed strategies to multiclass TSC problems. But this paper mainly focuses on the theoretical evidences and some advantages of the proposed strategies. Table II shows details of data sets and hyperparameter selections of the SIST model.

B. Experimental results

This subsection will show advantages of the proposed strategies by comparing the SIST algorithm with the state-of-the-art algorithms in terms of accuracy and efficiency. The purpose of the proposed strategies is reducing the time complexity with little loss of the accuracy achieved by the state-of-the-art on binary TSC problems. Hence, at first, it should be checked that the SIST model indeed achieves a top classification accuracy on most of binary TSC problems.

Table III shows the accuracy comparison between the SIST model and the state-of-the-art models on the data sets. The accuracy of the compared models comes from the TSC society. Researchers strictly selected the hyperparameters of these compared algorithms and made the classification results as accurate as they can. According to the table, the SIST model performs best on more than a half of the data sets. Actually, on the data sets except for ‘SonyAIBORobotSurface’, the accuracy of the SIST model is fairly close to the best accuracy.

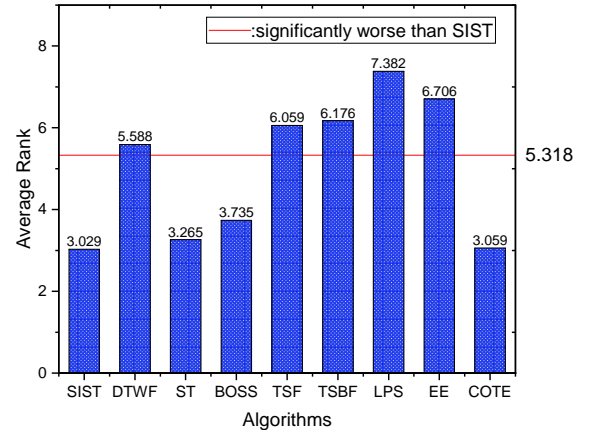


Fig. 8. Average accuracy rank and Friedman test with 95% confidence. The average rank in this figure is the arithmetic mean of the accuracy ranks on all the experimental data sets. The red cut line in this figure is the threshold calculated by the Friedman test.

More details about the accuracy comparison can be seen in Fig 8. In this figure, all the models’ average ranks are depicted. By putting these average ranks in the same histogram, there is a holistic view of the comparison between the SIST model and the compared models. According to the data in this figure, it can be judged whether the SIST model is significantly better than the compared models by the Friedman test with a 95% confidence. The red cut line in the figure is a threshold calculated according to the Friedman test. The compared models with an average rank larger than the threshold are significantly worse than the SIST model. In Fig 8, the red cut line goes across the bars of the DTWF, the TSF, the TSBF, the LPS, and the EE, which means average ranks of those five models are larger than the threshold. Hence, those five models are significantly worse than the SIST model in terms of classification accuracy. The left four models are the ST, the BOSS, the COTE, and the SIST. And they are in the same level in terms of the classification accuracy. Though the SIST model is not significantly better than the ST, the BOSS, and the COTE in the Friedman test with a 95% confidence, the average rank of the SIST model is still smaller than the average ranks of those three models. Hence, the SIST model is at least not worse than the ST, the BOSS, and the COTE in terms of the classification accuracy.

Based on the above experimental evidences and analysis, the ST, the BOSS, the COTE, and the SIST can be presently regarded as the first tier candidates of the TSC algorithms in terms of the classification accuracy. Next, the efficiency comparison among the first-tier algorithms will be focused on. Because the purpose of the proposed strategies are reducing the time complexity with little loss of the accuracy achieved by the state-of-the-art, the precondition that keeping the accuracy achieved by the state-of-the-art is more important. Some algorithms may possess the lower time consumption, but they can not keep a high accuracy. And keeping the precondition is exactly what the theoretical evidences in this paper work for.

TABLE I
HYPERPARAMETER SET

delete overlap shapelet	true, false
shapelet length	3,4
left and right relaxation factor	3,4
shapelet number	10,50,100,250,500,750,1000,1250,1500,2000

TABLE II
DATA ATTRIBUTES AND HYPERPARAMETERS CHOSEN BY 10-FOLD CROSS VALIDATION

Data Attribute			Hyperparameter of SIST			
Dataset	Train\Test	Length	Delete Overlap	Shapelet Length	L\R Relaxation Factor	Shapelet Number
Coffee	28\28	286	true	3	3\3	10
DistalPhalanxOutlineCorrect	600\276	80	true	4	4\4	2000
Earthquakes	322\139	512	true	3	3\3	10
ECG200	100\100	96	true	3	4\3	1500
ECGFiveDays	23\861	136	false	3	3\3	2000
GunPoint	50\150	150	false	4	3\3	1250
Ham	109\105	431	true	3	4\3	50
Herring	64\64	512	true	4	4\3	10
ItalyPowerDemand	67\1029	24	false	3	4\4	100
MiddlePhalanxOutlineCorrect	600\291	80	true	3	4\4	1500
MoteStrain	20\1252	84	true	4	3\4	250
ProximalPhalanxOutlineCorrect	600\291	80	true	4	3\3	2000
SonyAIBORobotSurface1	20\601	70	false	4	4\3	50
SonyAIBORobotSurface2	27\953	65	false	3	3\3	2000
Strawberry	613\370	235	false	4	4\4	1250
TwoLeadECG	23\1139	82	true	3	4\3	50
Wine	57\54	234	true	3	3\3	250

Hence, the efficiency comparison focuses only on the first-tier candidates.

The time consumption plays an important role for the practical application of algorithms. Table IV shows the time consumption comparison on all the experimental data sets in the same hardware and software environment. Since these four algorithms are all eager learning algorithms, the time consumption is mainly spent in training classifier. Hence, the time shown in Table IV is the training time. From the result in Table IV, it can be seen that no matter what the experimental data set is, the SIST has the lowest time consumption. The SIST model has evident advantage compared with the ST, the BOSS and the COTE in terms of time consumption, which shows the run time advantage the proposed strategies bring. In this table, the COTE, which is hot on the heels of the SIST in Fig 8, has a fairly large training time. To some extent, the huge training time of the COTE makes some troubles in the practical application. On some data sets, the training time of

the COTE is more than some days, whereas the SIST only spend some minutes in getting a similar classification result. On some data sets, the training time of the compared first-tier algorithms may be some hours or some minutes, whereas the SIST model only spends some seconds. All the data shown in Table IV tells that the SIST prevails in the four first-tier algorithms in terms of the run time, which implies the power of the proposed strategies.

Next, a further comparison about the efficiency is conducted. By defining the product of the train set size and the data length as the scale of a data set, the experimental data sets are sorted into three categories according to their scales. Then the average accuracy and the average training time of these four compared algorithms are depicted in the coordinate system. Fig 9 shows the concrete results. three kinds of data sets correspond to three graphs in Fig 9. The vertical axis represents the average accuracy and the horizontal axis represents the average training time. It should be noticed that

TABLE III
ACCURACY COMPARISON ON BINARY DATASETS WITH EIGHT TOP TSC ALGORITHMS

Dataset	DTWF	ST	BOSS	TSF	TSBF	LPS	EE	COTE	SIST
Coffee	0.973	0.995	0.989	0.989	0.982	0.95	0.989	1.000	1.000
DistalPhalanxOutlineCorrect	0.796	0.829	0.815	0.810	0.816	0.767	0.768	0.804	0.830
Earthquakes	0.748	0.737	0.746	0.747	0.757	0.668	0.735	0.747	0.871
ECG200	0.819	0.840	0.891	0.868	0.847	0.808	0.881	0.873	0.86
ECGFiveDays	0.907	0.955	0.983	0.922	0.849	0.840	0.847	0.986	0.978
GunPoint	0.964	0.999	0.994	0.961	0.965	0.972	0.974	0.992	0.967
Ham	0.795	0.808	0.836	0.795	0.711	0.685	0.763	0.805	0.838
Herring	0.609	0.653	0.605	0.606	0.591	0.549	0.566	0.632	0.875
ItalyPowerDemand	0.948	0.953	0.866	0.958	0.926	0.914	0.914	0.970	0.978
MiddlePhalanxOutlineCorrect	0.798	0.815	0.808	0.794	0.800	0.770	0.782	0.801	0.897
MoteStrain	0.891	0.882	0.846	0.874	0.886	0.917	0.875	0.902	0.889
ProximalPhalanxOutlineCorrect	0.829	0.881	0.867	0.847	0.861	0.851	0.839	0.871	0.900
SonyAIBORobotSurface1	0.884	0.888	0.897	0.845	0.839	0.842	0.794	0.899	0.839
SonyAIBORobotSurface2	0.859	0.924	0.889	0.856	0.825	0.851	0.870	0.960	0.877
Strawberry	0.970	0.968	0.970	0.963	0.968	0.963	0.959	0.963	0.959
TwoLeadECG	0.958	0.984	0.985	0.842	0.910	0.928	0.959	0.983	0.982
Wine	0.892	0.926	0.912	0.881	0.879	0.884	0.887	0.904	1.000

TABLE IV
TIME COMPARISON ON BINARY DATASETS AMONG THE FIRST-TIER ALGORITHMS WITH THE SAME ACCURACY LEVEL (CPU : INTEL(R) CORE(TM) I7-6500U CPU @ 2.50GHZ ; RAM : 8GB ; OPERATING SYSTEM : WINDOWS 10 X64)

DataSet	ST	BOSS	COTE	SIST
Coffee	6.3s	6.6s	9.5E+03s	0.8s
DistalPhalanxOutlineCorrect	9.5E+03s	91.8s	2.9E+05s	91.4s
Earthquakes	1.5E+03s	1.6E+03s	9.1E+05s	110.2s
ECG200	64.5s	5.0s	1.3E+04s	3.0s
ECGFiveDays	7.6s	1.1s	1.1E+03s	0.9s
GunPoint	16.2s	3.4s	7.0E+03s	1.8s
Ham	51.1s	133.7s	2.8E+05s	8.0s
Herring	15.3s	66.2s	1.8E+05s	7.0s
ItalyPowerDemand	16.7s	0.6s	88.3s	0.5s
MiddlePhalanxOutlineCorrect	1.3E+05s	101.5s	2.5E+05s	36.9s
MoteStrain	4.7s	0.5s	151.8s	0.4s
ProximalPhalanxOutlineCorrect	9.8E+03s	78.3s	2.6E+05s	53.8s
SonyAIBORobotSurface1	2.0s	0.5s	114.2	0.4s
SonyAIBORobotSurface2	4.6s	1.0s	212.8s	0.8s
Strawberry	1.0E+04s	790.5s	5.3E+05s	295.4s
TwoLeadECG	4.4s	0.6s	283.0s	0.4s
Wine	11.2s	9.0s	4.3E+04s	1.5s

the average training time is dealt with a logarithmic function basing 10. That's because the difference of the average training time is too big to depict them in a coordinate system. Hence, the horizontal distance is not uniform or even. The real time difference increases exponentially as the horizontal distance grows linearly in the coordinate system.

In this figure, it can be seen that firstly the average accuracy of all the compared algorithms declines as the scale of data sets inclines. Secondly, no matter what the scale of data sets are, the SIST algorithm has the lowest average training time while the COTE algorithm has the highest one. Thirdly, on the data sets with a scale more than $1E + 04$, the SIST algorithm has the best average accuracy as well as the lowest average training time. Fourthly, as the scale of data sets increases, both the time advantage and the accuracy advantage of the SIST algorithm are increasingly obvious. Fifthly, there is no algorithm dominating the SIST algorithm in all the three graphs of Fig 9.

According to those discoveries in Table IV and Fig 9, the SIST algorithm indeed possesses an evident efficiency advantage on binary TSC problems. The supporting factors of the SIST algorithm are the two proposed strategies, and the SIST model is just a primary application of the proposed strategies on binary TSC problems. Therefore, the advantages of the proposed strategies can be seen in these experiments.

V. CONCLUSION AND FUTURE WORK

In this paper, two strategies are proposed to solve the time complexity problem of the ensemble ST algorithm. The main contributions are the theoretical evidences guaranteeing the effectiveness of these two strategies. Here, the word 'effectiveness' means that reducing the time complexity with the near-lossless accuracy achieved by the state-of-the-art. To show the power of these two strategies, the SIST model is proposed as a model implementation of them. The SIST model is specific to binary TSC problems, and some experimental evidences of the SIST model illustrate the advantages of the two strategies. Supported by the theoretical evidences, the two strategies actually have some generality in algorithms based on the shapelet transform. Hence, the future work of this paper is trying to apply these two strategies to more circumstances such as multiclass classification, semi-supervised learning and so forth. In the future, stronger theoretical evidences will also be explored to improve the theory system of these strategies of shapelet transform algorithms.

REFERENCES

- [1] E. J. Keogh and S. Kasetty, "On the need for time series data mining benchmarks: A survey and empirical demonstration," *Data Mining and Knowledge Discovery*, vol. 7, pp. 349–371, 2002.
- [2] A. Apostolico, M. E. Bock, and S. Lonardi, "Monotony of surprise and large-scale quest for unusual words," *Journal of computational biology : a journal of computational molecular cell biology*, vol. 10 3-4, pp. 283–311, 2002.
- [3] E. J. Keogh, L. Wei, X. Xi, S.-H. Lee, and M. Vlachos, "Lb'keogh supports exact indexing of shapes under rotation invariance with arbitrary representations and distance measures," in *VLDB*, 2006.
- [4] A. Gionis and H. Mannila, "Finding recurrent sources in sequences," in *RECOMB*, 2003.

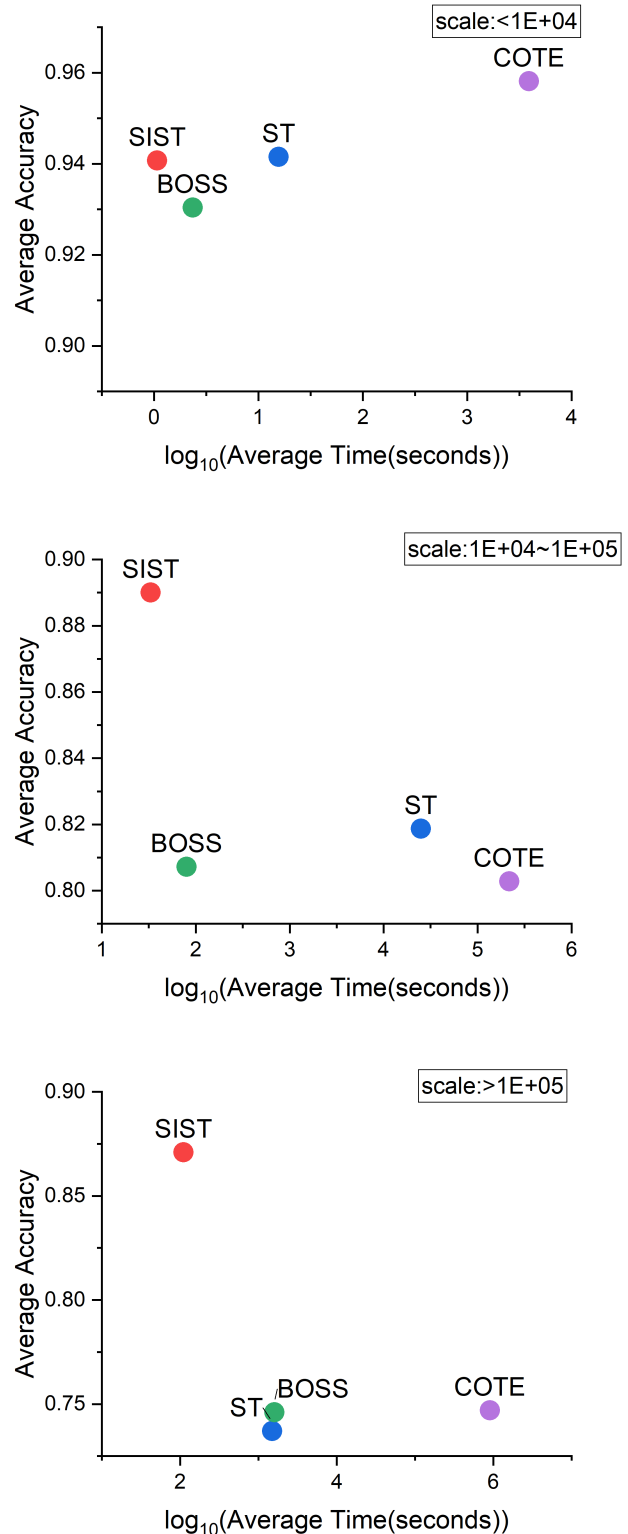


Fig. 9. Time-Accuracy comparison on data sets of different scale (scale is the product of train set size and data length)

- [5] A. Bagnall, J. Lines, A. Bostrom, J. Large, and E. J. Keogh, "The great time series classification bake off: a review and experimental evaluation of recent algorithmic advances," *Data Mining and Knowledge Discovery*, vol. 31, pp. 606–660, 2016.
- [6] J. Mei, M. Liu, Y.-F. Wang, and H. Gao, "Learning a mahalanobis distance-based dynamic time warping measure for multivariate time series classification," *IEEE Transactions on Cybernetics*, vol. 46, pp. 1363–1374, 2016.
- [7] T. Rakthanmanon, B. J. L. Campana, A. Mueen, G. E. A. P. A. Batista, M. B. Westover, Q. Zhu, J. Zakaria, and E. J. Keogh, "Addressing big data time series: Mining trillions of time series subsequences under dynamic time warping," *TKDD*, vol. 7, pp. 10:1–10:31, 2013.
- [8] Y. Jeong, M. K. Jeong, and O. A. Omitaomu, "Weighted dynamic time warping for time series classification," *Pattern Recognition*, vol. 44, pp. 2231–2240, 2011.
- [9] P.-F. Marteau, "Time warp edit distance with stiffness adjustment for time series matching," *IEEE Transactions on Pattern Analysis and Machine Intelligence*, vol. 31, pp. 306–318, 2009.
- [10] A. Stefan, V. Athitsos, and G. Das, "The move-split-merge metric for time series," *IEEE Transactions on Knowledge and Data Engineering*, vol. 25, pp. 1425–1438, 2013.
- [11] T. Górecki and M. Luczak, "Non-isometric transforms in time series classification using dtw," *Knowl.-Based Syst.*, vol. 61, pp. 98–108, 2014.
- [12] G. E. A. P. A. Batista, E. J. Keogh, O. M. Tataw, and V. M. A. de Souza, "Cid: an efficient complexity-invariant distance for time series," *Data Mining and Knowledge Discovery*, vol. 28, pp. 634–669, 2013.
- [13] T. Górecki and M. Luczak, "Using derivatives in time series classification," *Data Mining and Knowledge Discovery*, vol. 26, pp. 310–331, 2012.
- [14] J. Lines and A. Bagnall, "Time series classification with ensembles of elastic distance measures," *Data Mining and Knowledge Discovery*, vol. 29, pp. 565–592, 2014.
- [15] S. Roychoudhury, M. F. Ghalwash, and Z. Obradovic, "Cost sensitive time-series classification," in *ECML/PKDD*, 2017.
- [16] H. Deng, G. C. Runger, E. Tuv, and V. Martyanov, "A time series forest for classification and feature extraction," *Inf. Sci.*, vol. 239, pp. 142–153, 2013.
- [17] M. G. Baydogan, G. C. Runger, and E. Tuv, "A bag-of-features framework to classify time series," *IEEE Transactions on Pattern Analysis and Machine Intelligence*, vol. 35, pp. 2796–2802, 2013.
- [18] M. G. Baydogan and G. C. Runger, "Time series representation and similarity based on local autopatterns," *Data Mining and Knowledge Discovery*, vol. 30, pp. 476–509, 2015.
- [19] L. Ye and E. J. Keogh, "Time series shapelets: a novel technique that allows accurate, interpretable and fast classification," *Data Mining and Knowledge Discovery*, vol. 22, pp. 149–182, 2010.
- [20] E. J. Keogh and T. Rakthanmanon, "Fast shapelets: A scalable algorithm for discovering time series shapelets," in *SDM*, 2013.
- [21] J. Grabocka, N. Schilling, M. Wistuba, and L. Schmidt-Thieme, "Learning time-series shapelets," in *KDD*, 2014.
- [22] J. Lin, E. J. Keogh, L. Wei, and S. Lonardi, "Experiencing sax: a novel symbolic representation of time series," *Data Mining and Knowledge Discovery*, vol. 15, pp. 107–144, 2007.
- [23] P. Schäfer and U. Leser, "Fast and accurate time series classification with weasel," in *CIKM*, 2017.
- [24] J. Lin, R. Khade, and Y. Li, "Rotation-invariant similarity in time series using bag-of-patterns representation," *Journal of Intelligent Information Systems*, vol. 39, pp. 287–315, 2012.
- [25] P. Senin and S. Malinchik, "Sax-vsm: Interpretable time series classification using sax and vector space model," *2013 IEEE 13th International Conference on Data Mining*, pp. 1175–1180, 2013.
- [26] P. Schäfer, "The boss is concerned with time series classification in the presence of noise," *Data Mining and Knowledge Discovery*, vol. 29, pp. 1505–1530, 2014.
- [27] P. Smyth, "Clustering sequences with hidden markov models," in *NIPS*, 1996.
- [28] M. Corduas and D. Piccolo, "Clustering and classification by the autoregressive metric," 2013.
- [29] H. Chen, F. Tang, P. Tiño, and X. Yao, "Model-based kernel for efficient time series analysis," in *KDD*, 2013.
- [30] A. J. Bagnall and G. J. Janacek, "A run length transformation for discriminating between auto regressive time series," *J. Classification*, vol. 31, pp. 154–178, 2014.
- [31] R. J. Kate, "Using dynamic time warping distances as features for improved time series classification," *Data Mining and Knowledge Discovery*, vol. 30, pp. 283–312, 2015.
- [32] J. Hills, J. Lines, E. Baranauskas, J. Mapp, and A. Bagnall, "Classification of time series by shapelet transformation," *Data Mining and Knowledge Discovery*, vol. 28, pp. 851–881, 2013.
- [33] A. Bostrom and A. Bagnall, "Binary shapelet transform for multi-class time series classification," *T. Large-Scale Data- and Knowledge-Centered Systems*, vol. 32, pp. 24–46, 2015.
- [34] A. Bagnall, J. Lines, J. Hills, and A. Bostrom, "Time-series classification with cote: The collective of transformation-based ensembles," *IEEE Transactions on Knowledge and Data Engineering*, vol. 27, pp. 2522–2535, 2015.
- [35] J. Lines, S. Taylor, and A. Bagnall, "Hive-cote: The hierarchical vote collective of transformation-based ensembles for time series classification," *2016 IEEE 16th International Conference on Data Mining (ICDM)*, pp. 1041–1046, 2016.
- [36] A. Sharabiani, H. Darabi, A. Rezaei, S. Harford, H. Johnson, and F. Karim, "Efficient classification of long time series by 3-d dynamic time warping," *IEEE Transactions on Systems, Man, and Cybernetics: Systems*, vol. 47, pp. 2688–2703, 2017.
- [37] A. Mueen, E. J. Keogh, and N. E. Young, "Logical-shapelets: an expressive primitive for time series classification," in *KDD*, 2011.
- [38] L. Hou, J. T. Kwok, and J. M. Zurada, "Efficient learning of timeseries shapelets," in *AAAI*, 2016.
- [39] R. C. Guido, "Fusing time, frequency and shape-related information: Introduction to the discrete shapelet transform's second generation (dst-ii)," *Information Fusion*, vol. 41, pp. 9–15, 2018.
- [40] A. Bostrom, A. Bagnall, and J. Lines, "Evaluating improvements to the shapelet transform," 2016.